Physical CHEMISTRY

An Indian Journal

Full Paper

Gas sensitivity of cobalt-, molybdenum- and palladium-modified nanostructured SnO$_2$ films

S.M.Malyovanyi, O.I.Milovanova, E.V.Panov*

Vernadskii Institute of General & Inorganic Chemistry of the Ukrainian NAS, 32/34 Acad. Palladina ave., 03680 Kyiv, (UKRAINE)

E-mail : panov@ionc.kiev.ua

ABSTRACT

Co$_3$O$_4$-, MoO$_3$- and Pd-doped nanocrystalline SnO$_2$ powders have been synthesized in a nitrate melt. The phase composition, microstructure, morphology, fineness and distribution of dopant have been studied by XRD, TEM, SEM, EDX. The sensitivity S of films of these powders to a number of alcohols (methanol, ethanol, propanol, butanol, isoamyl alcohol) and dimethylketone has been studied by electrical conductivity measurement. The effect of doping (increase in S) is due to the formation of the nanocomposite SnO$_2$/dopant, in which the dopant either facilitates oxygen activation (Pd) or is an incomplete-oxidation (MoO$_3$, Co$_3$O$_4$) catalyst.   © 2015 Trade Science Inc. - INDIA

INTRODUCTION

"Chemical resistors" based on films of doped SnO$_2$ powders, whose electrical conductivity is very sensitive to the adsorption of gas molecules on their surface, are widely used in toxic and explosive gas sensors[1]. The main functional disadvantage of SnO$_2$-based sensors is their low selectivity[2]. To increase it, doping of SnO$_2$ with other oxides is employed. The doping efficiency increases if a nanocomposite of the base oxide SnO$_2$ and a dopant M are formed, catalysts (platinum metals or d-metal oxides) being used as dopants[2]. This approach allows one to increase the adsorption activity of SnO$_2$ and the oxidation rate of gas molecules on the SnO$_2$/M composite. Another peculiarity of the SnO$_2$/M composite is that the grain boundary between SnO$_2$

and M grains is very sensitive to the composition, microstructure of dopant and the nature (topography) of its distribution[3].

The procedure for the synthesis of the SnO$_2$/M nanocomposite for the detection of a particular gas involves a purely empirical approach. This is due to the specific character of gas-sensor reactions. For such reactions on thick films (i.e. prepared from synthesized SnO$_2$/M powders), the known established principles of heterogeneous catalysis theory can only be employed with ill-founded assumptions.

Known methods for the synthesis of SnO$_2$/M: chemical precipitation, sol-gel and solid-phase synthesis and others are better studied experimentally. For the products obtained by these methods, the correlation between synthesis and the physicochemical and functional properties of the synthesis product

Full Paper

SnO_2/M has been roughly studied. Of the functional properties, the effect of dopant on microstructure and hence on reactivity in the case of interaction with gases of different nature was considered as the most important one. Since the conclusions drawn in these studies did not give comprehensive answers as to the principles of selecting dopants for the desired selective gas reaction, we proposed an alternative method for the synthesis of SnO_2/M-based gas-sensitive material.

The developed method for the synthesis[4] of SnO_2/M nanocrystals in salt melts enables one to produce powders which differ in some properties (structure, phase composition, fineness, etc) from those obtained by known methods. Therefore, it is interesting to perform a comparative evaluation of data on the capabilities of materials synthesized in melts and commonly used materials of SnO_2/M type in the case of reactions, studied earlier, with atmospheric oxygen and gases-reductants.

This paper presents results on the synthesis of SnO_2/M nanocrystals (M=Co_3O_4, MoO_3, Pd, Sb_2O_5) in the $NaNO_3$-KNO_3 melt, their properties, the gas sensitivity of films of them in low-molecular alcohol (R-OH, R=CH_3, C_2H_5, C_3H_7, etc) and acetone vapor. The chosen dopants are two types of catalysts: platinum metals and d-metal oxides. Sb oxide was added when it was necessary to increase the electrical conductivity of SnO_2/M films (to reduce the testing error).

EXPERIMENTAL

The SnO_2 powders were produced by the interaction of $SnCl_2 \cdot 2H_2O$ precursor and dopants in the $NaNO_3$-KNO_3 melt (250-450 °C). $SbCl_3 \cdot 5H_2O$, $PdCl_2$, $Co(NO_3)_3$, $(NH_4)_6Mo_7O_{24}$ and sodium formate were used as the precursors of dopants. The morphology, microstructure, phase and chemical composition were studied by SEM (JEOL JSM – 6060-LA), TEM (JEOL JEM2010), the X-ray analyzers of these microscopes, an X-ray diffractometer (DRON-3M). The grain size d (nm) of doped SnO_2/M powders was estimated from the broadening of reflections in X-ray diffraction patterns using the Scherrer formula. The films of SnO_2/M powders

were prepared by the thick-film technology by applying a paste of powder in colloidal solution of ethylcellulose in terpineol to dielectric substrates of Al_2O_3-based ceramic with Ag electrodes. The resulting SnO_2/M films were dried at 100 °C for one hour and heat-treated at 550 °C. The response of the resistance R of such films in the time t (R-t) was measured at direct current with a UT61E multimeter with software for real-time data output to a computer in the format of Excel tables. R was measured in a temperature range of 20-350 °C and a gas concentration range of 0.5-350 ppm. The gas sensitivity S of films was analyzed (S=R_a/R_g; R_a – electrical resistance of SnO_2/M film in air, R_g – the same in analyte gas).

RESULTS AND DISCUSSION

Identification of synthesized powders. According to X-ray diffraction data (Figure 1), all obtained SnO_2/M samples (M=Co_3O_4, MoO_3, Pd) are single-phase ones, their diffraction patterns correspond to the standard (96-500-0225, tin (IV) oxide, cassiterite) and rutile structure (SnO_2).

It can also be seen that the samples synthesized in the $NaNO_3$-KNO_3 melt at 450 °C and without additional heat treatment have a satisfactory crystallinity. It will be recalled that the absence of heat
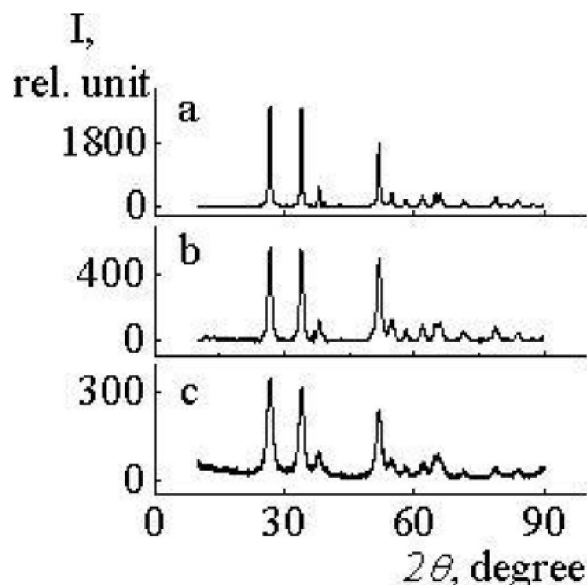

Figure 1 : X-ray diffraction patterns of SnO_2 (a), SnO_2/ 10 mol % MoO_3 (b), $Sn_{0.97}Sb_{0.03}O_2$/5 at % Pd (c) powders; CuKα-radiation

treatment (T>700 °C, 6-24 h) allows one to prevent such unwanted phenomena as SnO_2 recrystallization, oxidation of dopants, breakdown of dopant clusters because of their diffusion into the bulk of SnO_2 grain. The peaks in the diffraction patterns of all powders are highly broadened, indicating nanosized fraction of synthesized powders. Using the Scherrer formula, the mean size of the coherent-scattering region has been determined from the broadening of peaks. For SnO_2 powders, we obtained d=33 nm, for SnO_2/Pd d=6.2 nm; in the case of SnO_2/MoO_3, d depended on the MoO_3 concentration and varied between 33 and 11 nm over the range 0-10 mol % MoO_3. An analysis of data[5] showed that this nature of d variation may mean segregation of the dopant phase (MoO_3) with smaller d on the base oxide grain surface, i.e. formation of the SnO_3/MoO_3 nanocomposite. Because of the broadening of diffraction peaks, the SnO_2 unit cell constants a and c cannot be determined with required accuracy for different molybdenum concentrations, i.e. the possibility of formation of a SnO_2-dopant solid solution cannot be ruled out or confirmed. The formation of the SnO_2/MoO_3 composite is indirectly confirmed by the absence of Mo peaks up to the concentration 20 mol % MoO_3 from our X-ray diagrams[5] and those presented in[6] and by a decrease in the concentration of conduction electrons because of their interaction with surface Mo^{6+} ions to form Mo^{5+} ions and anion vacancies. The presence of Mo^{5+} ions in the SnO_2/MoO_3 composite was observed in EPR spectra of these powders[7].

Pd clusters were observed in high-resolution TEM images of SnO_2/Pd[8]. The size of SnO_2/M crystals and their agglomerates and their morphology are shown in Figure 2 for $Sn_{0.97}Sb_{0.03}O_2$/3 mol % MoO_3 as an example.

Values of d, which are close to XRD data, for powders with Pd can be seen in Figure 2b; the Pd content of the sample is 2.3 % (according to TEM analyzer data), i.e. is close to that preassigned in synthesis. The composition of $Sn_{0.97}Sb_{0.03}O_2$ powders is fairly uniform: the tin and oxygen content determined from four 50 × 50 μm windows of $Sn_{0.97}Sb_{0.03}O_2$/3mol% MoO_3 powder is close to the expected one (Figure 2c).

Gas sensitivity of the electrical conductivity of SnO_2-based thick films

SnO_2 films. A high resistance R_a of SnO_2 film in air and its decrease (down to R_g) with increasing alcohol vapor concentration in the gas-air mixture were observed (see inset in Figure 3a). Decrease in R for the gas-air mixture and its return to the initial value in air (Figure 3) are typical of alcohols (gases-reductants) and mean alcohol oxidation on the SnO_2 oxide catalyst chemisorbed by atmospheric oxygen.

Several alcohol oxidation mechanisms are possible[6]. Methanol oxidizes on SnO_2 to formaldehyde[6]. For other alcohols, the oxidation mechanism depends on the acidity of groups on the oxide surface. More basic groups provide the mechanism of alcohol dehydrogenation to form acetaldehyde and
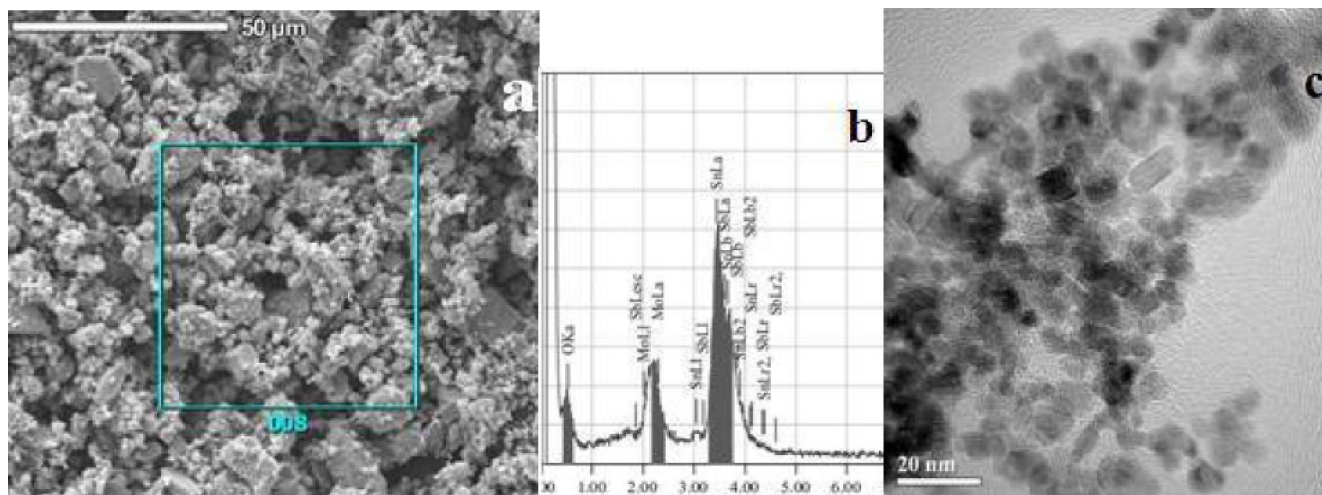

Figure 2 : SEM-image (a) and EDX-spectrum (b) of $Sn_{0.97}Sb_{0.03}O_2$/3 mol % MoO_3 powder and TEM-image (c) of $Sn_{0.97}Sb_{0.03}O_2$/2,5 % Pd powder
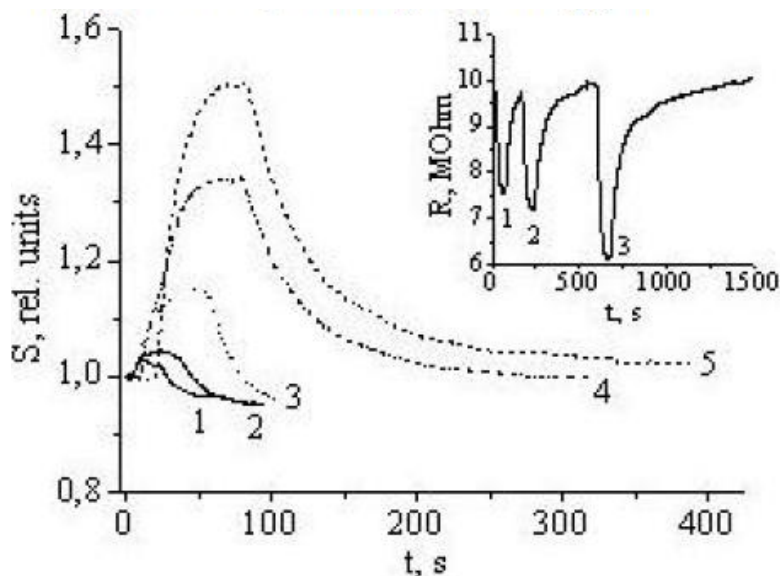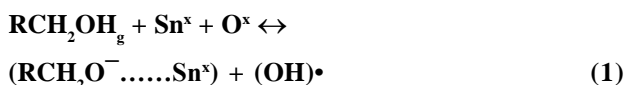
Figure 3 : Sensitivity S (R$_a$/R$_g$) of a SnO$_2$ film to alcohol vapor with a concentration of 3 ppm: (1) methanol, (2) propanol, (3) ethanol, (4) butanol, (5) isoamyl alcohol; the inset shows the dynamics of resistance variation (R-t) of a SnO$_2$ film at the butanol vapor concentration: (1) 1 ppm, (2) 3 ppm, (3) 5 ppm
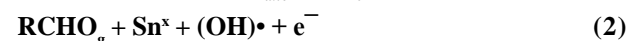
to give up electrons of this reaction to the SnO$_2$ conduction band, which leads to a decrease in R down to R$_g$ on alcohol vapor inflow. The kinetics of this gas reaction differ widely in the order: methanol, ethanol, propanol, butanol, isoamyl alcohol and depend not only on the difference in reaction products (formaldehyde, acetaldehyde) and reactive forms of oxygen involved in it, but also on the difference in the degree of carbon chain branching (steric factor). Apparently because of this we have S ~ 1 and unstable R$_a$ values in the case of methanol; for butanol and isoamyl alcohol we have S ~ 1.5, a good reproducibility of R$_a$ and R$_g$ and proportionality of S to alcohol vapor concentration (Figure 3).

To account for the dependence of S on the size and structure of R-OH alcohol carbon chain (R=CH$_3$, C$_2$H$_5$, C$_3$H$_7$, etc), some data on heterogeneous catalysis should be employed. In terms of the acid-base model of the formation of catalytic and adsorption centers on the SnO$_2$ surface, which has basic properties, the oxidative dehydrogenation reaction of alcohols[6, 9], which proceeds according to the two-step scheme:

Dissociative alcohol adsorption from the gas phase:

$$RCH_2OH_g + Sn^x + O^x \leftrightarrow$$
$$(RCH_2O^- \ldots\ldots Sn^x) + (OH) \bullet \qquad (1)$$

And hydrogen elimination from the carbon atom:

$$(RCH_2O^- \ldots.. Sn^x) + O_{a\pi c}^- + V_o \rightarrow$$
$$RCHO_g + Sn^x + (OH)\bullet + e^- \qquad (2)$$

Is preferable, where Sn^x, O^x are tin and oxygen atoms in the SnO$_2$ lattice, V$_o$ is oxygen vacancies, and (OH)·is hydroxo-group on the tin dioxide surface.

According to this scheme, all lower alcohols oxidize on SnO$_2$ to RCHO aldehydes, except methanol, which oxidizes to formaldehyde. RCHO and CH$_2$O can be further oxidized to CO$_2$ and H$_2$O.

The mechanism of dehydrogenation according to the scheme (1, 2) leads to the transfer of dehydrogenation reaction electrons to the SnO$_2$ conduction band, i.e. forms the response S of the sensor. The dehydrogenation reaction rate apparently increases with carbon chain length. It can be seen (Figure 4) that for butanol and isoamyl alcohol, S>1.4 (for methanol, ethanol and propanol, S~1.0), i.e. the process of hydrogen elimination from the carbon atom is promoted with carbon chain extension.

This experimental fact (Figure 3, curves 4 and 5) indicates the dehydrogenation mechanism to predominate in our experiment. There is a difference of the sensing properties of our SnO$_2$ from those of SnO$_2$ obtained by known methods, e.g. by chemical precipitation[6]. Unlike our case, S decreases in the lat-
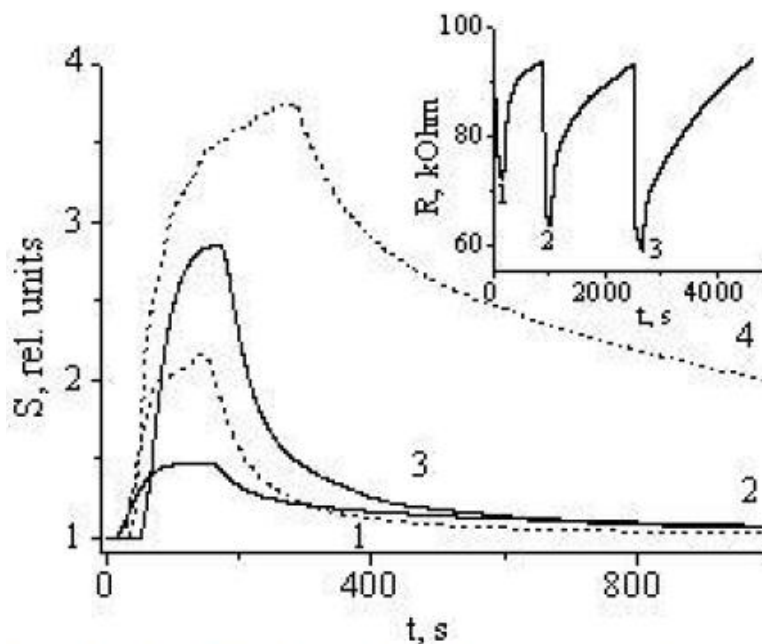
Figure 4 : Sensitivity S (R_a/R_g) of a $Sn_{0.97}Sb_{0.03}O_2/5$ at % Pd film to alcohol vapor with a concentration of 3 ppm: (1) ethanol, (2) butanol, (3) methanol, (4) isoamyl alcohol; the inset shows the dynamics of resistance variation (R-t) of a $Sn_{0.97}Sb_{0.03}O_2/5$ at % Pd film at the butanol vapor concentration: (1) 1 ppm, (2) 3 ppm, (3) 5 ppm

ter in going to propanol and butanol. This decrease is accounted for[6] by steric effect as a result of replacement of linear radical by branched one (butanol). It is yet unclear why the steric factor is not realized on the surface of SnO_2 synthesized in a salt melt reaction medium.

$Sn_{0.97}Sb_{0.03}O_2/5$ at % Pd film. Figure 4 shows R-t plots for methanol, ethanol, butanol, isoamyl alcohol. The following distinguishes them from the plots shown in Figure 3 for SnO_2: much (3-4 times) higher $S=R_a/R_g$ for methanol and isoamyl alcohol (which differ greatly in the number of carbon atoms and structure), no influence of dopant on the S value for butanol, independence of S from the isoamyl alcohol concentration.

The doping of SnO_2 powders with Pd, if its clusters are formed on the SnO_2 surface, can perform three functions: alcohol oxidation reaction catalysis (1), dissociative adsorption of O_2 molecule on the SnO_2 surface (2), interaction between Pd clusters and the SnO_2 matrix, as a result of which a change in the configuration of palladium d electrons[2] and new reaction properties of the SnO_2 surface are possible. These consequences of doping with Pd for ethanol and acetone were observed in[8], though no direct proofs of the doping mechanism were obtained.

Since the oxidation mechanisms and products (formaldehyde and acetaldehyde) for methanol and isoamyl alcohol differ, the following scheme of dopant influence is possible: a slight increase in the surface concentration of oxygen in the active O^- form owing to the dissociative chemisorption of O_2 molecules on Pd clusters.

This conclusion agrees with the independence of conduction electron concentration from isoamyl alcohol concentration (Figure 4). This means that there is some saturation of S, which is due to the limit of active centers (oxygen in the O_2^- and O^- form) for the alcohol oxidation reaction.

An analysis of a large body of experimental data on the gas sensitivity of SnO_2 showed[10] that there is no general approach to the choice of dopant-catalyst for selective reaction. When solving this problem, the method of varying the properties of dopants and their concentration in the SnO_2 matrix/dopant nanocomposite proved to be effective. In order to check the capabilities of this method and to specify the mechanism of action of dopants-catalysts, the nanocomposites SnO_2/Pd (0.2-2.5 at %), SnO_2/0.2 at % Pd + 1.0 mol % MoO_3, SnO_2/MoO_3 (1-10 mol %), $Sn_{0.97}Sb_{0.03}O_2$/1.0 mol % Co_3O_4 have been studied additionally.

Full Paper

SnO$_2$/0.2 at % Pd film. For the gas mixture of acetone and ethanol vapor with argon, the sensitivity of the material is the same as for pure SnO$_2$: the S value is small and is larger for ethanol (Figure 5a). These properties are accounted for by the fact that ethanol (or acetone) interacts with oxygen in the O$_2^-$ form, which is usually present on pure SnO$_2$, is stable at 200 °C and is desorbed only at T>300 °C when O$^-$ takes its place[10], i.e. we have the same effect as for SnO$_2$ in air. On the SnO$_2$/Pd composite in air, a reaction of dissociative adsorption of O$_2$ molecules on Pd clusters takes place[8], followed by the fixation of more reactive O$^-$ ions on the matrix (SnO$_2$) and participation of O$^-$ in oxidation reactions. In this case, not only the vapor sensitivity S, but also the kinetics of oxidation reactions improve, which is corroborated by a great reduction in response and recovery time (Figure 5b).

SnO$_2$/0.2 at % Pd. + 1 mol % MoO$_3$ film. In this case, a small amount of MoO$_3$ as an oxidation reaction catalyst was added to the above sensor material, palladium retaining the function of generator of the active oxygen form O$^-$. The limitation of the amount of MoO$_3$ is caused by the fact that its addition to SnO$_2$ increases greatly the electrical resistance of SnO$_2$ film[5] and reduces thereby the accuracy of its measurement. The testing of the SnO$_2$/Pd + MoO$_3$ film with acetone, ethanol and butanol vapor showed its high ethanol sensitivity (S~6, Figure 5b and S~100, Figure 6) and very high butanol sensitivity (S~1.5, Figure 4 and S~250, Figure 6) as

compared with low acetone sensitivity (S~4, Figure 6). A very short time of response of film R to analyte vapor is also observed (Figure 6).

The observed behavior of the parameter S of the SnO$_2$/Pd + MoO$_3$ composite cannot be accounted for by the individual capabilities of Pd and MoO$_3$ as oxidation catalysts. The interaction mechanism of the electron subsystems of composites SnO$_2$/Pd and SnO$_2$/MoO$_3$ must be considered in greater detail. The effect of change in the configuration of Pd and MoO$_3$ d electrons as a result of interaction between these clusters and the SnO$_2$ matrix, pointed out in[2, 10], has, perhaps a crucial influence on the parameter S.

SnO$_2$/MoO$_3$ film. The electrophysical properties of SnO$_2$ and MoO$_3$ crystals (SnO$_2$ and MoO$_3$ are n-type semiconductors) are sensitive to alcohol and ketone vapor. Each of the oxides has a low sensitivity S to these gases. For SnO$_2$, this can be seen in Figure 3, and for MoO$_3$, S is still lower[6]. The composition of the SnO$_2$/MoO$_3$ nanocomposite increases slightly S at a MoO$_3$ content as low as 4 mol % and ten times as much at a concentration of 10 mol %. The most explicable cause of the increase in S in going from individual SnO$_2$ and MoO$_3$ nanocrystals to their nanocomposite is the dominating role of just the grain boundary between SnO$_2$ and MoO$_3$ in the conduction mechanism. The grain boundary is especially sensitive[10] to the adsorption of oxygen and alcohol vapor; gas reactions, which change the surface concentration of conduction electrons, n$_s$, and the value of the interfacial potential barrier V$_s$, pri-
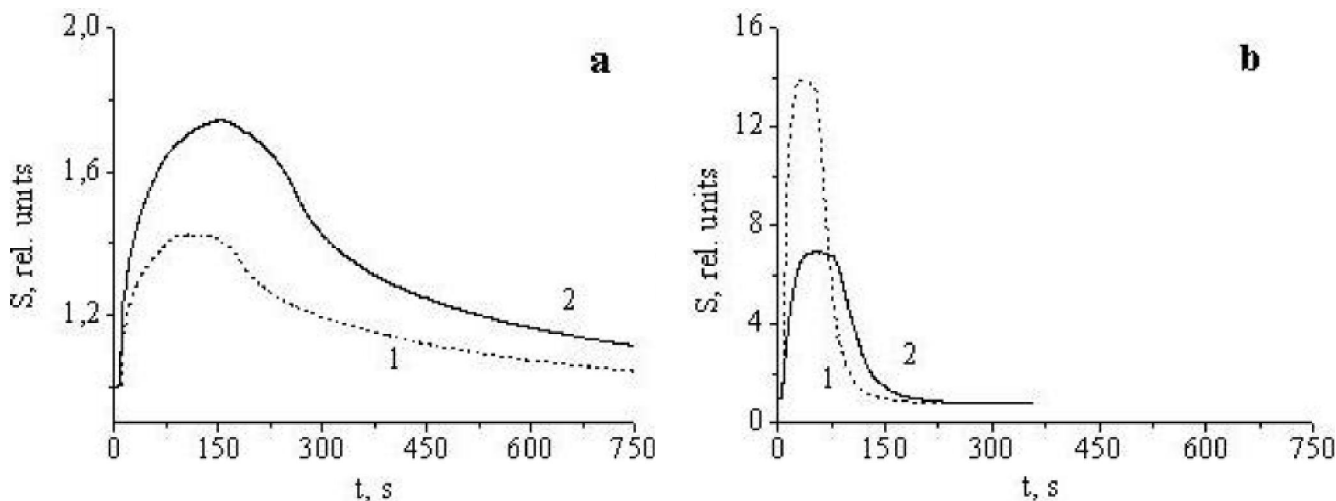

Figure 5 : Sensitivity S (R$_a$/R$_g$) of a SnO$_2$ / 0.2 at % Pd film to acetone (1) and ethanol (2) vapor with a concentration of 350 ppm in argon (a) and in air (b)
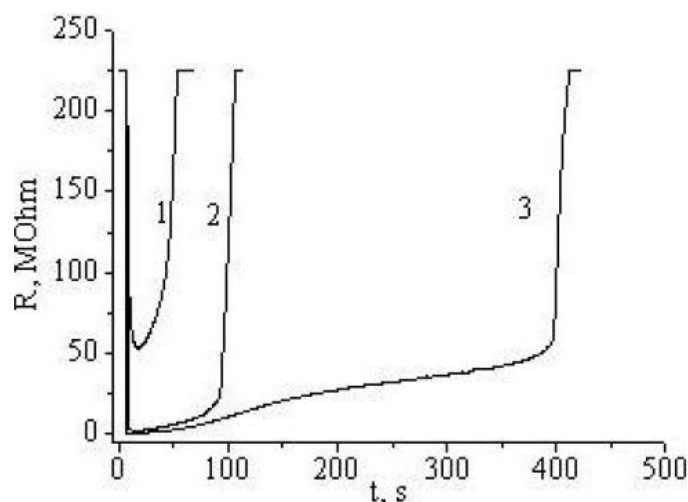
Figure 6 : Dynamics of resistance variation (R-t) of a SnO$_2$/0.2at%Pd+1mol%MoO$_3$ film to analyte vapor with a concentration of 550 ppm: (1) acetone, (2) ethanol, (3) butanol

marily occur at it. The parameters n$_s$ and V$_s$ control the conductivity of the SnO$_2$/M composite. The value of n$_s$ in SnO$_2$ apparently varies under the MoO$_3$ cluster; the barrier V$_s$ is formed not by the same interface charges (in the case of SnO$_2$ grains alone), but by charges which differ for SnO$_2$ and MoO$_3$. This scheme of the SnO$_2$/MoO$_3$ interface (compared with SnO$_2$/SnO$_2$ grain contacts) must lead to an increase in S[10]. This S increase mechanism in the case of doping SnO$_2$ is impossible if a SnO$_2$-dopant solid solution is formed instead of composite[6]. The obtained data on S behavior for SnO$_2$/MoO$_3$ do not account for the great increase in S in the case of the SnO$_2$/Pd+MoO$_3$ composite. Here, electrophysical mechanisms of ~100-fold S enhancement act besides chemical factors (adsorption and oxidation catalysts, i.e. Pd and MoO$_3$).

An important characteristic of sensor material is the optimum temperature of the gas sensitivity S. It is individual for the material prepared by a definite synthesis method, its composition, structure and morphology. To assess these qualities, S-t plots for possible optimum temperatures of the sensor material are suitable (Figure 7).

It can be seen that the temperature factor, i.e. transition from the operating temperature 200 °C to 250 °C, allows one to realize the selectivity of the SnO$_2$/4mol%MoO$_3$ material for acetone (compare Figure 7a and Figure 7b). Raising the temperature to 300 °C does not practically change the acetone

sensitivity of SnO$_2$/MoO$_3$, but increases S by a factor of 4 for ethanol, i.e. rules out the use of the composite for the analysis of acetone in a mixture with ethanol. Besides, long operation of SnO$_2$/MoO$_3$ films at 300 °C results in the irreducibility of analysis results because of the chemical and structural degradation of the material.

SnO$_2$/1 mol % Co$_3$O$_4$ film. The dynamics of the sensitivity variation of a film based on the SnO$_2$/Co$_3$O$_4$ composite in the case of pulsed inflow of an air-ethanol (acetone) mixture into the film atmosphere are shown in Figure 8.

When analyzing these data, both the chemical and the electrophysical factors of the effect of dopant on the S value must be taken into account[13, 14]. The dopant Co$_3$O$_4$ participates as oxidation catalyst in the gas reaction. When S$_n$$^{4+}$ ions are substituted by Co^{2+} and Co^{3+} ions (from Co$_3$O$_4$) on the surface, new oxygen vacancies V$_0$, V$_0$-Co^{2+} complexes and positively charged holes are formed. V$_0$ and V$_0$-Co^{2+} increase the surface density of O$^-$ and O^{2-} ions, i.e. the density of reaction centers for the gas-reductant and hence the density of electron transfer from the gas reaction to the conduction band. In experiment (Figure 8), this effect leads to a 4-5-fold increase in S. The physical effect of doping results in a recombination of formed holes with existing electrons (at the SnO$_2$ and Co$_3$O$_4$ grain boundary), which leads to an increase in R at the grain boundary. Another physical effect of doping
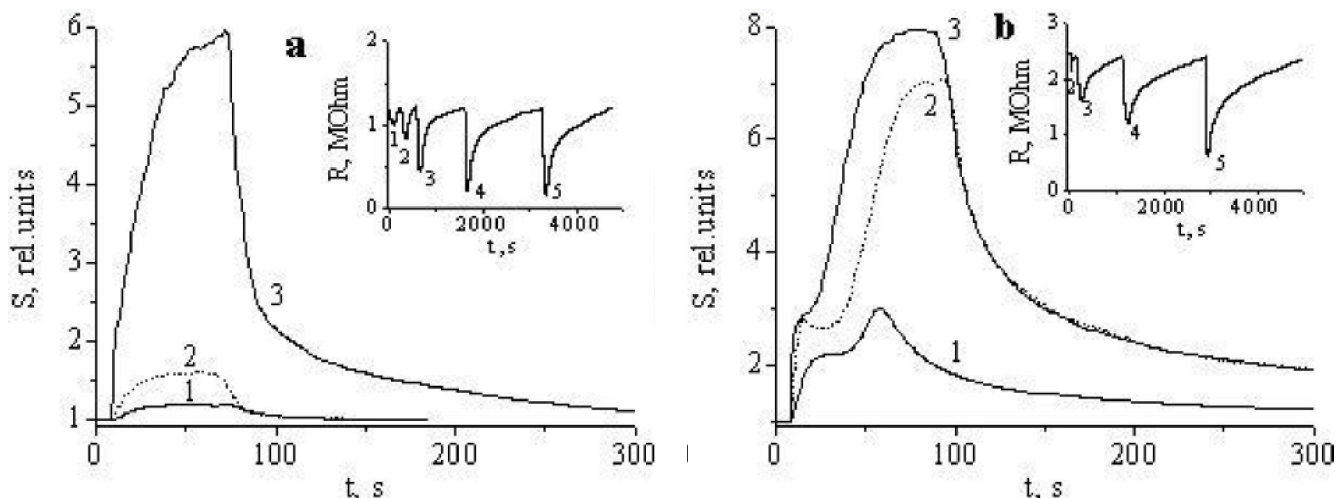
Full Paper

Figure 7 : Sensitivity S (R_a/R_g) of a SnO₂+4mol%MoO₃ film to ethanol (a) and acetone (b) vapor with a concentration of 350 ppm at different temperature: 1 – 200°C; 2 – 250°C; 3 – 300°C; the insets show the dynamics of resistance variation (R-t) of a SnO₂+4%Mo film at 200°C at the ethanol (a) and acetone (b) vapor concentration: 1 – 5 ppm; 2 – 10 ppm; 3 – 50 ppm; 4 – 100 ppm; 5 – 350 ppm
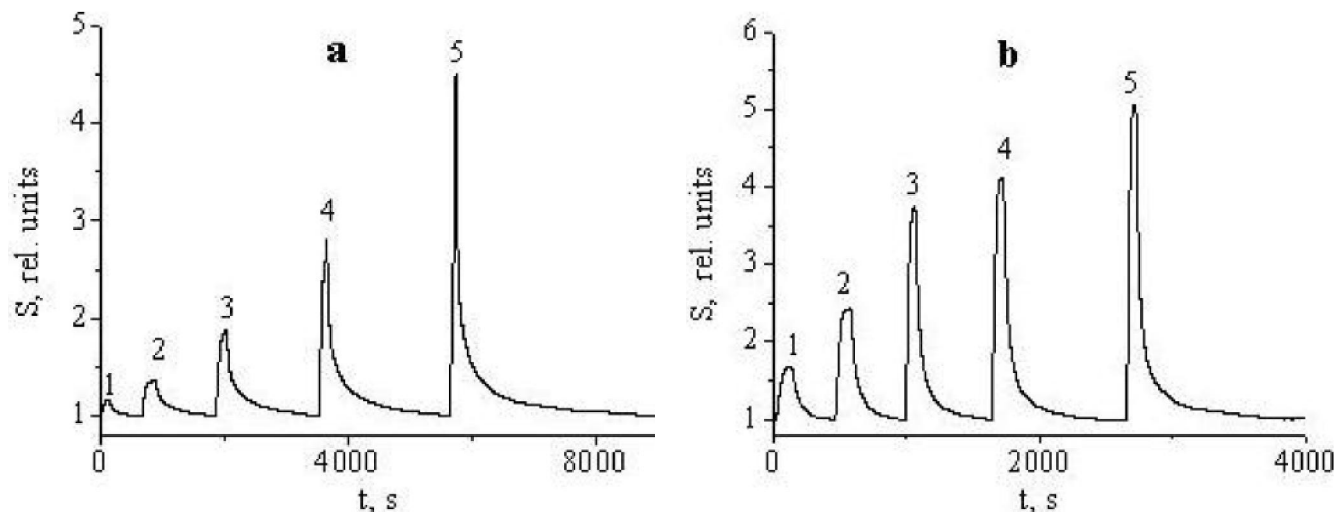

Figure 8 : Sensitivity S (R_a/R_g) of a $Sn_{0,97}Sb_{0,03}O_2$/1 mol% Co_3O_4 film at 200 °C to the acetone (a) and ethanol (b) vapor concentration: 1 – 5 ppm; 2 – 10 ppm; 3 – 50 ppm; 4 – 100 ppm; 5 – 350 ppm

is the appearance in the SnO₂ (n-type)/Co₃O₄ (p-type) composite of a p-n transition and its considerable influence on the S value for the following reasons. It is known[10] that adsorbed oxygen is localized at the grain boundary, enlarges the charged region and reduces thereby the conductivity in air. When the composite interacts with ethanol (acetone), Co₃O₄ is reduced and returns electrons to the SnO₂ conduction band. Thus, the combination of the chemical and electronic factors in the composite leads to a considerable decrease in film R and an increase in S for gases-reductants in going from pure SnO₂ to the SnO₂/Co₃O₄ composite,

which is confirmed experimentally (Figure 8). The films containing over 1 wt % Co have a high resistance and decreased gas sensitivity. This may be due to a high defect concentration because of Co³⁺ incorporation into the SnO₂ structure; the defects give rise to a high concentration of holes, which absorb SnO₂ conduction electrons. Unlike our SnO₂/Co₃O₄ thick films, an increase in R by the action of acetone was observed in thin films[14, 15]. In the latter case, the increase in intergranular potential barrier height and the contribution of the hole-electron recombination process were apparently deciding factors.

Full Paper

CONCLUSION

Nanocrystalline SnO_2 powders doped with Pd, MoO_3, Co_3O_4 have been synthesized in a nitrate melt. The mean particle size depends on the type and concentration of dopant and ranges between 6 and 33 nm (d=33 nm for SnO_2). At a dopant concentration of 1-2 %, the ethanol sensitivity S increases by a factor of ~250 for SnO_2/0.2 % Pd + 1 % MoO_3 (I) and 4-6 for SnO_2/Pd (II), SnO_2/MoO_3 (III), SnO_2/ Co_3O_4 (IV). For the samples II-IV, the obtained results agree with the existing concept of the mechanism of action of Pd, MoO_3, Co_3O_4 as catalysts: Pd activates the oxygen adsorbed on SnO_2; MoO_3 and Co_3O_4 are catalysts for the incomplete oxidation of simple organic compounds.

The electrical aspects of influence on S, which occur in the samples I and IV, remain unclear and call for special research. In the sample I in the vicinity of Pd and MoO_3 clusters, a change in the electrical properties of the matrix itself (SnO_2) is possible on the SnO_2 surface. It is on these portions that a gas oxidation reaction involving SnO_2 conduction electrons proceeds, i.e. in the case of the sample I, there must be a joint effect of the catalytic and electronic factors of doping on the S value. In the sample IV at the SnO_2 and Co_3O_4 grain boundary, a p-n transition appears which must be sensitive to the adsorption of gases. However, we did not observe this effect when measuring S.

In some investigations of low-molecular alcohols, a dependence of S on the hydrocarbon chain length must be observed. In[6] for SnO_2/MoO_3 samples obtained by precipitation from a solution, a dependence of S with maximum for propanol was observed. In our case for $Sn_{0.97}Sb_{0.03}O_2$/Pd samples (synthesized in a melt), the maximum values were obtained for methanol (the shortest chain) and isoamyl alcohol (the largest number of carbon atoms in the radical). This difference in the effect on S may be due not only to the difference in the properties of Pd and MoO_3 catalysts, but also to a noticeable difference in the microstructure and morphology of SnO_2 crystals synthesized in a nitrate melt.

REFERENCES

[1]   D.E.Williams; Sens.Actuators B, **57**, 1 **(1999)**
[2]   M.N.Rumyantseva, V.V.Kovalenko, A.M.Gaskov, T.Pagnier; Ross.Khim.Zhurn., (in Russian), **51**, 61 **(2007)**.
[3]   N.Barsan, D.Koziej, U.Weimar; Sens.Actuators B, **121**, 18 **(2007)**
[4]   S.M.Malyovanyi, E.A.Genkina, E.V.Panov; Physics and Technology of Surface, (in Russian), **13**, 152 **(2007)**.
[5]   E.V.Panov, O.I.Milovanova, S.M.Malyovanyi; Ukr.chem.j., (in Russian), **81**, 48 **(2015)**.
[6]   E.A.Makeeva, M.N.Rumyantseva, A.M.Gaskov; J.Inorg.Chem., (in Russian), **41**, 442 **(2005)**.
[7]   M.Ivanovskaya, P.Bogdanov, G.Faglia, P.Nelli; Sens.Actuators B, **77**, 268 **(2001)**.
[8]   E.V.Panov, O.I.Milovanova, S.M.Malyovanyi, E.A.Genkina; Chemistry, Physics and Technology of Surface, (in Russian), **5**, 309 **(2014)**.
[9]   H.Idriss, E.G.Seebauer; J.Mol.Catal.A., **152**, 201 **(2000)**.
[10] G.Korotcenkov; Sens.Actuators B, **107**, 209 **(2005)**.
[11] Z.A.Ansari, S.G.Ansari, T.Ko, J.H.Oh.; Sens.Actuators B, **87**, 105 **(2002)**.
[12] J.Arbiol, J.R.Morante, P.Bouvier, T.Pagnier, E.A.Makeeva, M.N.Rumyantseva, A.M.Gaskov.; Sens.Actuators B, **133**, 144 **(2008)**.
[13] Ming-Ming Zhang, Gua-Shun Jiang; Chinese J.Chemical Physics, **20**, 315 **(2007)**.
[14] Shriram B.Patil, P.P.Patil, Mahendra A.Moreb; Sens.Actuators B, **125**, 126 **(2007)**.
[15] G.Korotchenkov, I.Boris, V.Brinzari, S.H.Han, B.K.Cho; Sens.Actuators B, **182**, 112 **(2013)**.